

# A “Shake ‘n Bake Route” to Functionalised Zr-UiO-66 Metal-Organic Frameworks

Roberto D’Amato<sup>#†</sup> Roberto Bondi<sup>#</sup>, Intissar Moghdad<sup>||</sup> Fabio Marmottini<sup>#</sup>, Matthew J. McPherson<sup>ç</sup>, Houcine Naïli<sup>§</sup>, Marco Taddei<sup>ç\*</sup> and Ferdinando Costantino<sup>#\*</sup>

<sup>#</sup>Dipartimento di Chimica Biologia e Biotecnologia, University of Perugia, Via Elce di Sotto 8, 06123 Perugia, Italy.  
Email:ferdinando.costantino@unipg.it

<sup>ç</sup> Energy Safety Research Institute, Swansea University, Fabian Way, Swansea SA1 8EN, United Kingdom

<sup>||</sup>Laboratory of Advanced Materials, National Engineering School, Sfax University, P.B. 1173, 3038 Sfax, Tunisia

<sup>§</sup> Laboratory Physico Chemistry of the Solid State, Department of Chemistry, Faculty of Sciences of Sfax, P.B. 1171, 3000 Sfax, Sfax University, Tunisia.

<sup>\*</sup>Dipartimento di Chimica e Chimica Industriale, Università di Pisa Via Giuseppe Moruzzi, 13 - 56124 - Pisa (Italy).  
Email:marco.taddei@unipi.it

---

**ABSTRACT:** We report a novel synthetic procedure for the high-yield synthesis of metal-organic frameworks with UiO-66 topology starting from a range of commercial Zr<sup>IV</sup> precursors and various substituted dicarboxylic linkers. The syntheses are carried out by grinding in a ball mill the starting reagents, namely Zr salts and the dicarboxylic linkers, in the presence of a small amount of acetic acid and water (1 mL total volume for 1 mmol of each reagent), followed by incubation at either room temperature or 120 °C. Such a “shake ‘n bake” procedure avoids the use of large amounts of solvents generally used for the syntheses of Zr-MOF. Acidity of the linkers and the amount of water are found to be crucial factors in affording materials of quality comparable to that of products obtained in solvo- or hydrothermal conditions.

---

## Introduction

The development of green and scalable procedures for the synthesis of metal-organic frameworks (MOFs) is currently considered the main factor to enable widespread industrial application and commercialization of these materials.<sup>1,2</sup> The focus is primarily on the production of highly stable MOFs at low cost, in high yield and fulfilling most of the requirements of sustainability and atom economy.<sup>3,4</sup> Zirconium-based MOFs (Zr-MOFs) are currently considered benchmark materials for their high chemical and thermal stability, structural versatility and employment in a vast range of applications, ranging from gas separation,<sup>5–7</sup> catalysis,<sup>8,9</sup> water sorption,<sup>10,11</sup> proton conductivity<sup>12</sup> and drug delivery.<sup>13</sup> Their structure is based on the different connectivity of hexanuclear clusters of formula Zr<sub>6</sub>O<sub>4</sub>(OH)<sub>4</sub><sup>12+</sup> with polytopic carboxylic linkers, designing MOFs with variable degrees of connectivity and topologies, such as fcu (UiO-66 and

MOF-801), csq (NU-1000), reo (DUT-67) and spn (MOF-808).<sup>14–17</sup> Other topologies based on different SBUs, such as dodecanuclear clusters, were also recently reported.<sup>18</sup> Zr-MOFs are often prepared employing hazardous solvents with high boiling points such as N,N-dimethylformamide (DMF), strong acids and soluble chloride or nitrate metal salts.<sup>19</sup> A remarkable effort has been recently made for ensuring safer and cleaner procedures for the synthesis of MOFs by using different approaches able to minimize the use of hazardous reagents and solvents with high boiling points and the generation of large amounts of waste byproducts.<sup>20,21,22,23,24</sup>

Mechanochemistry is a well-established approach for performing clean and fast syntheses of a wide range of compounds, including metal-organic materials, avoiding common solvothermal routes and maximizing the atom economy.<sup>25</sup> In particular, liquid assisted grinding (LAG) or ionic-liquid assisted grinding (ILAG) are efficient procedures that make use of a small amount of solvents and/or metal-oxide precursors to enhance the crystallization kinetics.<sup>26</sup> Accelerated aging is another solvent-free route which takes advantage of the relatively high vapour pressure of small amounts of organic solvents.<sup>27,28</sup> Mechanochemical routes have recently been developed for the synthesis of many Zr-MOFs.<sup>29</sup> In particular, the use of templating agents, water-based LAG and extrusion resulted in the synthesis of Zr-MOFs of different topologies with high yield and high purity.<sup>30</sup> However, in order to attain the desired phase, preformed Zr<sub>6</sub>O<sub>4</sub>(OH)<sub>4</sub><sup>12+</sup> or Zr<sub>12</sub>O<sub>8</sub>(OH)<sub>8</sub><sup>24+</sup> clusters already assembled with monocarboxylic ligands, such as acetate or methacrylate, are normally used.<sup>30,31,32</sup> These clusters are often prepared using wet chemistry routes, adding a preliminary synthetic step to the procedure. Huang et al.<sup>29</sup> recently reported the ultrarapid (3 min) water-based LAG synthesis of nanocrystalline perfluorinated UiO-66 starting from a preformed

methacrylate cluster and tetrafluoroterephthalic acid (F4-BDC). The authors found that other linkers, such as terephthalic acid (BDC), 2-aminoterephthalic acid (NH<sub>2</sub>-BDC) and 2-bromoterephthalic acid (Br-BDC) failed to afford a crystalline product, attributing the higher reactivity of F4-BDC to its higher acidity, which enhances its solubility in water. Indeed, F4-BDC has recently been employed for the synthesis of UiO-66 type MOFs in water, even at room temperature.<sup>33–36</sup> Notably, Ye et al.<sup>37</sup> recently reported on a simple method to produce UiO-66 in high yield by grinding ZrOCl<sub>2</sub>·8H<sub>2</sub>O and BDC and subsequently heating the resulting mixture at 130 °C for 12 hours. Attempts using ZrCl<sub>4</sub> and Zr(NO<sub>3</sub>)<sub>4</sub>·5H<sub>2</sub>O as precursors failed to afford a crystalline product.

Inspired by these works, we set out to combine these two approaches to investigate the synthesis of a range of functionalised UiO-66 analogues. An initial screening of different commercially available salts, namely, Zr(NO<sub>3</sub>)<sub>4</sub>·5H<sub>2</sub>O, ZrOCl<sub>2</sub>·8H<sub>2</sub>O, ZrO(NO<sub>3</sub>)<sub>2</sub>·4H<sub>2</sub>O and ZrCl<sub>4</sub> was first carried out. Further investigation on the influence of AcOH/H<sub>2</sub>O ratio on the crystallinity of the compounds was also done. This screening was performed on the compounds prepared with Zr(NO<sub>3</sub>)<sub>4</sub>·5H<sub>2</sub>O, which afforded materials with high yield and crystallinity. Acidity of the linkers was found to be responsible of the different reactivity and quality of the obtained MOFs.

## Experimental

### Chemicals

Zirconium nitrate pentahydrate (Zr(NO<sub>3</sub>)<sub>4</sub>·5H<sub>2</sub>O) and zirconium oxynitrate tetrahydrate (ZrO(NO<sub>3</sub>)<sub>2</sub>·4H<sub>2</sub>O) were supplied by Carlo Erba. Zirconium oxychloride octahydrate (ZrOCl<sub>2</sub>·8H<sub>2</sub>O) and 2-nitroterephthalic acid were supplied by Alfa Aesar. Zirconium chloride (ZrCl<sub>4</sub>), tetrafluoroterephthalic acid, 2-bromoterephthalic acid and acetic acid were supplied by Sigma Aldrich. 2,5-pyridinedicarboxylic acid and 2-aminoterephthalic acid were supplied by Merck-Millipore. Molecular structures and calculated pKa values of the carboxylic linkers are shown in figure 1.

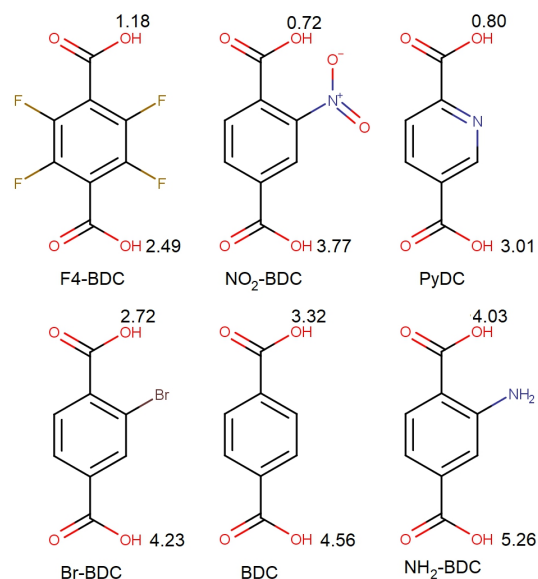


Figure 1. Molecular structure of the linkers used in this work. pKa values are also included next to the corresponding carboxylic groups. The values were calculated using the online tool Chemicalize (chemicalize.com).

### Synthetic procedures

Synthetic procedures were optimized in a stepwise manner. Initially, the different Zr salts were used as Zr source in the syntheses with F<sub>4</sub>-BDC ligand at RT and at 120 °C. The salt providing the best quality of the MOF was then chosen for the synthesis with the other linkers. Finally, a study on the influence of the AcOH/H<sub>2</sub>O ratio on the crystallinity and surface area as function of linker acidity was also carried out.

### Screening of Zr salts for the syntheses of F<sub>4</sub>-UiO-66 at RT and 120 °C

1 mmol of a zirconium salt (429 mg for Zr(NO<sub>3</sub>)<sub>4</sub>·5H<sub>2</sub>O; 322 mg for ZrOCl<sub>2</sub>·8H<sub>2</sub>O; 233 mg for ZrCl<sub>4</sub> and 303 mg for ZrO(NO<sub>3</sub>)<sub>2</sub>·4H<sub>2</sub>O) with 1 mmol of F<sub>4</sub>-BDC (238 mg) were put together in a agate vessel with a 0.5 cm ø agate ball. Acetic acid (AcOH, 1.0 mL, 17.5 mmol) was also added. The mixture was mechanically ground at 30 Hz for 15 min with a Fritsch planetary micro mill Pulverisette 7. The slurry was then recovered and left standing under a 25 mL beaker flipped upside down at RT for 24 h. For Zr(NO<sub>3</sub>)<sub>4</sub>·5H<sub>2</sub>O and ZrO(NO<sub>3</sub>)<sub>2</sub>·4H<sub>2</sub>O. For ZrO(NO<sub>3</sub>)<sub>2</sub>·4H<sub>2</sub>O the synthesis was performed at 120 °C by transferring the slurry to a 15 mL Teflon autoclave for 24 h. The obtained gel was separated by centrifugation and washed three times with deionised (DI) water and once with acetone. The solid was then dried in oven at 80 °C for 24 h. Yields: Zr(NO<sub>3</sub>)<sub>4</sub>·5H<sub>2</sub>O-RT = 92%; Zr(NO<sub>3</sub>)<sub>4</sub>·5H<sub>2</sub>O-120 = 93%; ZrOCl<sub>2</sub>·8H<sub>2</sub>O-RT = 90%; ZrCl<sub>4</sub>-RT = 85%; ZrO(NO<sub>3</sub>)<sub>2</sub>·4H<sub>2</sub>O-RT = 66%; ZrO(NO<sub>3</sub>)<sub>2</sub>·4H<sub>2</sub>O-120 = 90%.

## Syntheses of X-UiO-66 (X = NH<sub>2</sub>, Br, NO<sub>2</sub>, Py)

For the synthesis of Br-UiO-66 and NH<sub>2</sub>-UiO-66, 1 mmol of Zr(NO<sub>3</sub>)<sub>4</sub>·5H<sub>2</sub>O (429 mg) and 1 mmol of the desired linker (181 mg for NH<sub>2</sub>-BDC, 245 mg for Br-BDC) were put into an agate vessel with a 0.5 cm ø agate ball. AcOH (0.9 mL, 15.7 mmol) and water (0.1 mL, 5.5 mmol) were added and the mixture was mechanically ground for 15 min with a Fritsch planetary micro mill Pulverisette 7 at 50 Hz. The slurry was then transferred to a 15 mL Teflon autoclave and heated at 120 °C for 24 h. The obtained gel was recovered and washed three times with DI water and once with acetone. The solid was then dried in an oven at 80 °C for 16 h. The synthesis of Br-UiO-66 was also performed by heating at 120 °C for 1 h. Yields: NH<sub>2</sub>-BDC-120 = 78%; Br-BDC-120 = 85%.

For the synthesis of NO<sub>2</sub>-UiO-66, 1 mmol of Zr(NO<sub>3</sub>)<sub>4</sub>·5H<sub>2</sub>O (429 mg) and 1 mmol of NO<sub>2</sub>-BDC (211 mg) were put into an agate vessel with a 0.5 cm ø agate ball, then AcOH (1.0 mL, 17.5 mmol) was added and the mixture was mechanically ground for 15 min with the Fritsch planetary micro mill Pulverisette 7 at 50 Hz. The slurry was then put under a beaker and left standing at RT for 24h. The same steps described above were then carried out. Yield: 86%.

In the case of PyDC, 1 mmol of linker (167 mg), 1 mmol of Zr(NO<sub>3</sub>)<sub>4</sub>·5H<sub>2</sub>O (429 mg) and 1 mL of concentrated HNO<sub>3</sub> (65%, 15.57 M, 15 mmol) were added to an agate vessel with a 0.5 cm ø agate ball, then the mixture was mechanically ground for 15 min with a Fritsch planetary micro mill Pulverisette 7 at 50 Hz. The resulting slurry was transferred to a 15 mL Teflon autoclave and heated at 120 °C for 24 h in an oven. The same steps described above were then carried out. The same synthesis was performed by heating at 120 °C for 1 h. Yield: 88%.

## Modulated syntheses of X-UiO-66 (X=F<sub>4</sub>, NO<sub>2</sub>, Br, NH<sub>2</sub>)

In order to investigate the modulator effect of water for the formation of clusters, various amounts of water (0-100 µL, 0-5.5 mmol) were added to an agate vessel with a 0.5 cm ø agate ball containing 1 mmol of Zr(NO<sub>3</sub>)<sub>4</sub>·5H<sub>2</sub>O (429 mg), 1 mmol of the desired linker (238 mg for F<sub>4</sub>-BDC, 211 mg for NO<sub>2</sub>-BDC, 245 mg for Br-BDC, 181 mg for NH<sub>2</sub>-BDC) and AcOH (1.0-0.9 mL, 17.5-15.7 mmol) in such a way that the total volume of liquids was kept equal to 1.0 mL. The mixture was mechanically ground for 15 min with a Fritsch planetary micro mill Pulverisette 7 at 50 Hz. For the synthesis of F<sub>4</sub>- and NO<sub>2</sub>-UiO-66 the slurry was then left standing under a beaker flipped upside down at RT for 24 h, while for the synthesis of Br- and NH<sub>2</sub>-UiO-66 the slurry was transferred to a 15 mL Teflon autoclave and heated at 120 °C for 24 h in an oven. The obtained gels were recovered and washed three times with DI water and once with acetone. The solids were then dried in oven at 80 °C for 16 h.

### Scaled-up synthesis of F<sub>4</sub>-UiO-66

*Step 1.* 4 mmol of Zr(NO<sub>3</sub>)<sub>4</sub>·5H<sub>2</sub>O (1.96 g) was ground together with F<sub>4</sub>-BDC (0.952 g) in a mortar. AcOH (10 mL, 1.75 mmol)

was added and the mixture was homogenised in the mortar. The slurry was then put under a beaker and left standing at RT for 24 h. The obtained gel was separated by centrifugation and washed three times with deionised (DI) water and once with acetone. The solid was then dried in oven at 80°C for 24 h. Yield: 1.5 g, 90%

*Step 2.* 10 mmol of Zr(NO<sub>3</sub>)<sub>4</sub>·5H<sub>2</sub>O (4.29 g) was ground together with 10 mmol of F<sub>4</sub>-BDC (2.38 g) in a mortar. AcOH (10 mL, 1.75 mmol) was added and the mixture was homogenised in the mortar. The slurry was then put under a beaker and left standing at RT for 24 h. The obtained gel was separated by centrifugation and washed three times with deionised (DI) water and once with acetone. The solid was then dried in oven at 80°C for 24 h. Yield: 3.9 g, 93%.

## Analytical procedures

Powder X-Ray Diffraction (PXRD). PXRD patterns were collected with a 40 s step<sup>-1</sup> counting time and with a step size of 0.016 ° 2θ on a PANalytical X'PERT PRO diffractometer, PW3050 goniometer, equipped with an X'Celerator detector by using the CuKα radiation. The long fine focus (LFF) ceramic tube operated at 40 kV and 40 mA.

Field Emission Scanning Electron Microscopy (FE-SEM). The morphology of the crystalline samples was investigated with a FEG LEO 1525 scanning electron microscope working with an acceleration voltage of 15 kV. Samples were preliminarily sputtered with a Cr coverage to enhance the conductivity.

Thermogravimetric analysis (TGA). TGA was performed using a Netzsch STA490C thermoanalyzer under a 20 mL min<sup>-1</sup> air flux with a heating rate of 10 °C min<sup>-1</sup>.

Nitrogen adsorption and desorption isotherms were collected using a Quantachrome Nova 2000e analyser or a Micromeritics ASAP 2010 analyser. Prior to the analysis, the samples were degassed overnight under dynamic vacuum at 120 °C. B.E.T. analysis and t-plot analysis of the adsorption data were used to calculate specific surface area and micropore volume, respectively. Harkins and Jura equation was used as reference for the statistical thickness calculation.

Nuclear magnetic resonance (NMR). Quantitative <sup>1</sup>H and <sup>19</sup>F-NMR analysis of hydrolysed solids was performed at 25 °C on a Bruker Avance II DRX400 instrument equipped with a BBFO broadband probe. About 10-20 mg of solid was introduced in a glass vial, which was kept in an oven at 120 °C for 2 h to remove most of residual water from the pores. The dry solid was then weighed and treated with 1 mL of a 1 M NaOH solution in D<sub>2</sub>O, spiked with either 0.11 M 2-fluorobenzoic acid (for samples containing F<sub>4</sub>-BDC) or 0.10 M fumaric acid (for samples containing NO<sub>2</sub>-BDC, Br-BDC and PyDC) as an internal standard. The mixture was briefly sonicated and left to digest overnight. The NMR tubes were then loaded with the solution, taking care to avoid transferring solid particles to the tubes. <sup>1</sup>H-NMR spectra were acquired by collecting 4 scans with acquisition time of 5 s and d1 of 10 s. <sup>19</sup>F-NMR spectra were acquired by collecting 4 scans with acquisition time of 3 s and d1 of 5 s.

## Results and Discussion

We started our investigation by screening different commercial  $Zr^{IV}$  precursors in combination with  $F_4$ -BDC, which was demonstrated by Huang et al.<sup>29</sup> to be very prone to rapidly form a UiO-66 phase when milled with preformed hexanuclear  $Zr^{IV}$  clusters. The syntheses were carried out by ball milling equimolar amounts of the  $Zr^{IV}$  precursor and  $F_4$ -BDC (1 mmol each) in a planetary ball mill with a 0.5 cm  $\phi$  agate ball in the presence of 1.0 mL of AcOH for 15 minutes. The resulting slurry was then transferred to a closed container and incubated at RT for 24 hours. The mixture was then washed with water and acetone to remove the unreacted reagents and centrifuged to recover the solid. Using these amounts of reagents and AcOH, a concentration of 1 M of both salt and linker was obtained, which is 10 to 40 times higher than that normally used for DMF- or water-based syntheses of UiO-66 type MOFs.<sup>30,35,38-40</sup> We obtained phase-pure and crystalline UiO-66 from  $Zr(NO_3)_4 \cdot 5H_2O$ ,  $ZrOCl_2 \cdot 8H_2O$  and  $ZrCl_4$  (Figure 2a). In the case of  $ZrO(NO_3)_2 \cdot 4H_2O$ , the mixture had to be heated to 120 °C in order to obtain a crystalline product (Figure 1S). The products obtained from  $Zr(NO_3)_4 \cdot 5H_2O$  and  $ZrOCl_2 \cdot 8H_2O$  displayed broad reflections around 4-5 °2 $\theta$ , which could be associated with the presence of defects.<sup>41</sup> No residual reflections of the linker were present in the PXRD patterns of the products, proving the efficacy of the workup procedure (Figure 2S). SEM micrographs show that MOF crystallites with ill-defined morphology and size in the nanometric range (below 100 nm) were formed (Figure 3S). The use of  $ZrCl_4$  afforded MOF with slightly lower yield and a lower degree of crystallinity and surface area respect to the other precursors, which could be due to the lack of crystallisation water in this salt. Given that 1.33 equivalents of water are needed to provide the oxide and hydroxide ions constituting the metal clusters, water is essential for the successful formation of the MOF. The fact that we still obtained the MOF using  $ZrCl_4$  suggests that the precursor did contain some water, due to its strong tendency to absorb humidity from the atmosphere, but the amount was not stoichiometric. The  $N_2$  adsorption-desorption isotherms at 77 K obtained with these samples are reported in Figure 2b and they can be classified as type I isotherms, which are typical of microporous materials. The specific surface area and micropore volumes were calculated from the Brunauer-Emmett-Teller (BET) and t-plot analyses of the adsorption data, respectively, and are reported in Table 1. The highest BET surface area of 802  $m^2 g^{-1}$  was recorded for the sample obtained from  $Zr(NO_3)_4 \cdot 5H_2O$ . This value is higher than that previously reported for perfluorinated UiO-66 synthesized in water.<sup>30,34</sup>

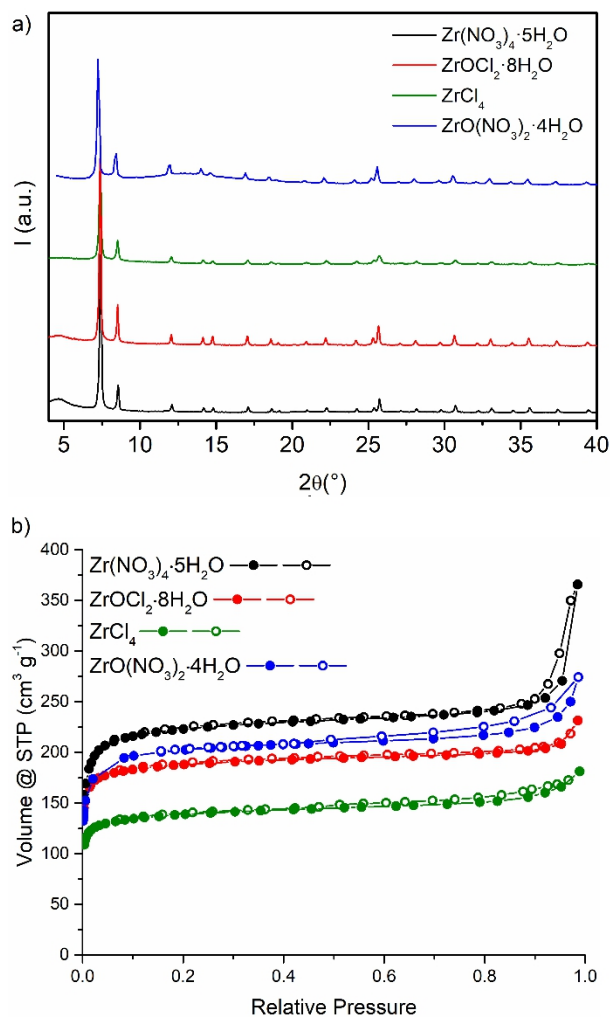


**Figure 2.** PXRD patterns (a) and  $N_2$  adsorption isotherms at 77 K (b) of the products obtained from the reaction of  $F_4$ -BDC with  $Zr(NO_3)_4 \cdot 5H_2O$  (black),  $ZrOCl_2 \cdot 8H_2O$  (red) and  $ZrCl_4$  (olive) at RT and with  $ZrO(NO_3)_2 \cdot 4H_2O$  at 120 °C (blue).

**Table 1.** BET surface area and micropore volume values for perfluorinated UiO-66 samples synthesized starting from different Zr precursors.

Precursor	Incubation temperature	BET surface area ( $m^2 g^{-1}$ )	Micropore Volume ( $cm^3 g^{-1}$ )
$Zr(NO_3)_4 \cdot 5H_2O$	RT	802	0.30
$ZrOCl_2 \cdot 8H_2O$	RT	750	0.27
$ZrCl_4$	RT	540	0.19
$ZrO(NO_3)_2 \cdot 4H_2O$	120 °C	783	0.30

Thermogravimetric analysis (TGA) showed that all products start decomposing at a similar temperature of 300 °C, consistent with what observed in previous literature reports (Figure 4S).<sup>1,34</sup> These results suggest that  $Zr(NO_3)_4 \cdot 5H_2O$  is the most suitable

precursor to obtain F<sub>4</sub>-UiO-66 with high crystallinity and porosity in mild conditions.

We then moved on to screen linkers bearing different functional groups. The same procedure described above was employed, using Zr(NO<sub>3</sub>)<sub>4</sub>·5H<sub>2</sub>O as the metal precursor and replacing F<sub>4</sub>-BDC with either NO<sub>2</sub>-BDC, Br-BDC, NH<sub>2</sub>-BDC, BDC or PyDC. However, a different behaviour, apparently depending on the acidity was observed for these linkers. Highly acidic linkers containing electron withdrawing groups (such as F<sub>4</sub>-BDC and NO<sub>2</sub>-BDC) afforded well crystallized MOFs in pure AcOH, whereas less acidic linkers containing electron donating groups (Br-BDC and NH<sub>2</sub>-BDC) were not able to successfully react in pure AcOH and needed a small amount of water in the synthesis to yield highly crystalline products. In order to gather additional insight on this aspect, we have performed a systematic screening of the influence of AcOH/H<sub>2</sub>O ratio in the crystallinity and porosity of the obtained products. The syntheses were then

performed by changing the amount of water from 0 μL (1 mL of pure AcOH) to 100 μL (900 μL AcOH/100 μL of H<sub>2</sub>O) with intermediate values (25, 50 and 75 μL). PXRD patterns, TGA analysis and N<sub>2</sub> adsorption isotherms of the samples obtained at different synthetic conditions are shown in figure 4S and 5S. Figure 3 shows the PXRD patterns of F<sub>4</sub> (a) NO<sub>2</sub> (b), Br (c) and NH<sub>2</sub> (d) -UiO-66 MOFs obtained at different water/AcOH ratio, whereas the BET surface area and micropore volumes are reported in table 2.

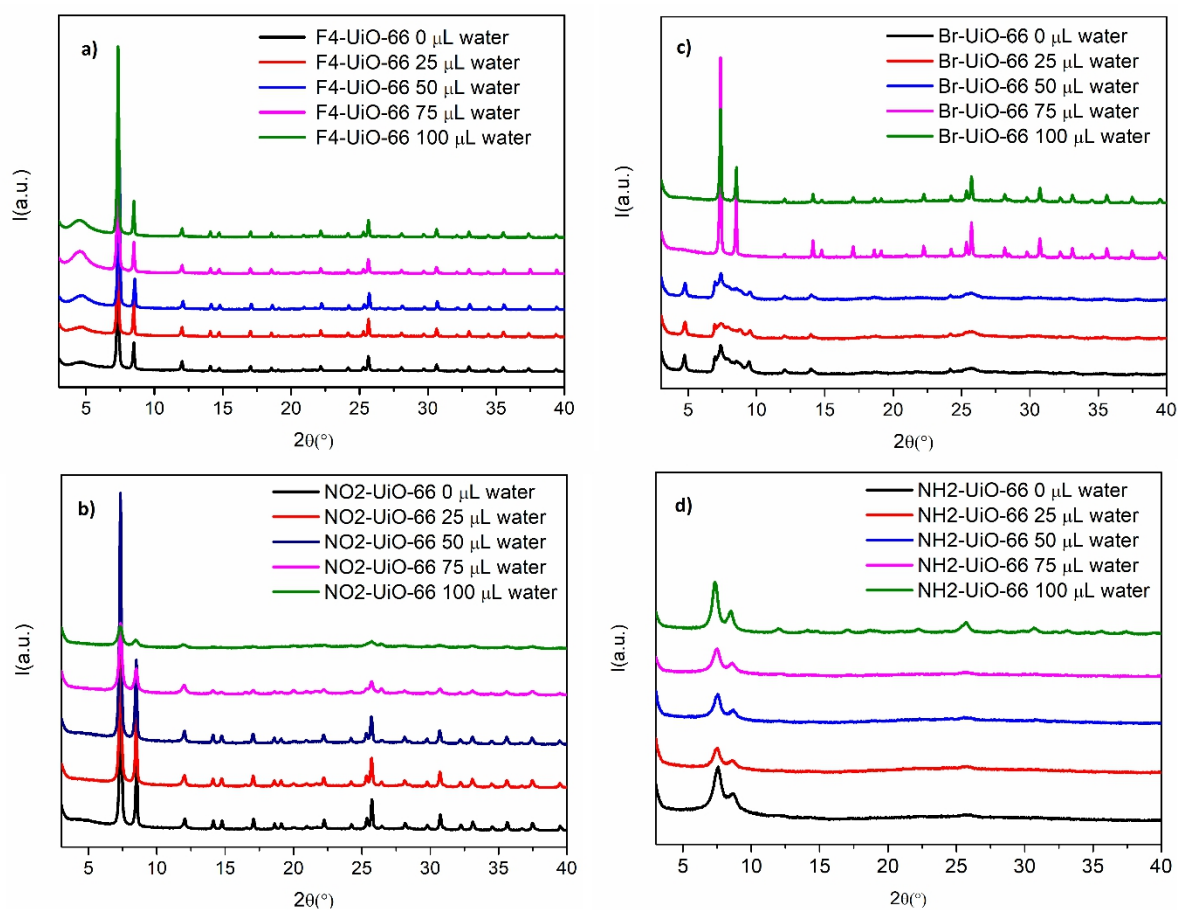


**Figure 3.** PXRD patterns of (a) F<sub>4</sub>-UiO-66, (b) NO<sub>2</sub>-UiO-66, (c) Br-UiO-66 and (d) NH<sub>2</sub>-UiO-66 synthesized changing the amount of water: 0 μL (black lines), 25 μL (red lines), 50 μL (blue lines), 75 μL (purple lines) and 100 μL (green lines).

**Table 2.** BET surface area and micropore for UiO-66 samples synthesized with different amounts of water, in addition to AcOH.

Sample	Amount of water	BET surface area (m <sup>2</sup> g <sup>-1</sup> )	Micropore volume (cm <sup>3</sup> g <sup>-1</sup> )
F <sub>4</sub> -UiO-66	0 μL	802	0.305
	50 μL	719	0.283
	100 μL	713	0.270
NO <sub>2</sub> -UiO-66	0 μL	793	0.303
	25 μL	758	0.292
	50 μL	630	0.242
Br-UiO-66	100 μL	724	0.282
NH <sub>2</sub> -UiO-66	100 μL	519	0.201

Sample	Solvent	BET surface area (m <sup>2</sup> g <sup>-1</sup> )	Micropore volume (cm <sup>3</sup> g <sup>-1</sup> )
Py-UiO-66	HNO <sub>3</sub> , 65%, 1 mL	979	0.361

F<sub>4</sub>-UiO-66 crystallisation seems to be little affected by the water/AcOH ratio, as all the PXRD patterns are indicative of highly crystalline compounds. An increase in the intensity of the broad reflection at low 2θ angle is observed at higher water amounts, which could indicate the presence of some defects. However, BET surface areas and micropore values appear to slightly decrease from 802 to 713 m<sup>2</sup> g<sup>-1</sup> as the water amount increases, which is not the expected effect for defective UiO-66 type MOFs.<sup>42</sup> Quantitative <sup>1</sup>H and <sup>19</sup>F NMR analysis of the digested MOFs (Figures 6S-8S) leads to determine the same chemical formula for samples prepared with 0 μL, 50 μL and 100 μL of water, i.e. Zr<sub>6</sub>O<sub>4</sub>(OH)<sub>4</sub>(F<sub>4</sub>-BDC)<sub>5.73</sub>(AcOH)<sub>0.54</sub>. The very low amount of AcOH retained in the framework suggests a small number of defects.

In the case of NO<sub>2</sub>-UiO-66, the trend is similar to F<sub>4</sub>-UiO-66, although the addition of 75 to 100 μL of water leads to a more evident loss of crystallinity and porosity respect to the samples obtained either in pure AcOH or with a lower amount of water (25-50 μL). The BET surface area of the sample obtained in pure AcOH is 793 m<sup>2</sup> g<sup>-1</sup>, in line with values found in the literature. Addition of 25 μL of water leads to a small decrease to 758 m<sup>2</sup> g<sup>-1</sup>, whereas upon addition of 50 μL of water the value drops to 630 m<sup>2</sup> g<sup>-1</sup>. Quantitative <sup>1</sup>H NMR analysis (Figures 9S-11S) suggests that samples prepared with 0 μL, 25 μL and 50 μL of water contain small amounts of defects, with representative formula Zr<sub>6</sub>O<sub>4</sub>(OH)<sub>4</sub>(NO<sub>2</sub>-BDC)<sub>5.75</sub>(AcOH)<sub>0.50</sub>. However, the discrepancy between the calculated mass composition based on the above formula and the experimental one derived from the absolute amounts through use of an internal standard suggests that the products contain some impurity, possibly of inorganic nature, and that the amount of such impurity increases with increasing amount of water used in the synthesis, thus accounting for the observed drop in BET surface area.

Concerning Br- and NH<sub>2</sub>-UiO-66, the trend observed so far is reversed: the products with higher crystallinity are those resulting from syntheses in the presence of a higher water quantity. This effect is more pronounced for Br-UiO-66, where the samples obtained with less than 75 μL of water display a different PXRD pattern from that of UiO-66, whereas samples obtained with 75 μL and 100 μL of water are highly crystalline, and the BET surface area (724 m<sup>2</sup> g<sup>-1</sup>) is consistent with that reported for conventional syntheses in DMF.<sup>38</sup> In this case, quantitative <sup>1</sup>H NMR analysis (Figure 12S) reveals the presence of a significant amount of AcOH and the proposed formula is Zr<sub>6</sub>O<sub>4</sub>(OH)<sub>4</sub>(Br-BDC)<sub>5.06</sub>(AcOH)<sub>1.88</sub>. Finally, NH<sub>2</sub>-UiO-66 was obtained in low crystallinity in all the syntheses, with a slight improvement for the sample made with 100 μL of water. Furthermore, the porosity of this product was much lower than that of the MOF obtained from a conventional synthesis in DMF.<sup>38,40,43,44</sup> Compared to the other linkers, NH<sub>2</sub>-BDC is by far the one less able to afford MOF of high quality. We also attempted syntheses employing bare BDC as the linker, consistently obtaining amorphous products, regardless of the amount of water used.

We speculate that the different behaviour displayed by different linkers is probably to be attributed to their acidity. As shown in Figure 1, pK<sub>a1</sub> values of BDC and NH<sub>2</sub>-BDC are 3.32 and 4.03, respectively, about one order of magnitude lower than that of Br-BDC (2.72) and more than two orders of magnitude lower than those of F<sub>4</sub>-BDC (1.18) and NO<sub>2</sub>-BDC (0.72). The effect can be two-fold: 1. BDC and NH<sub>2</sub>-BDC are not able to effectively deprotonate in reaction conditions, i.e. in the presence of an excess of a mild acid such as AcOH (pK<sub>a</sub> = 4.64); 2. since solubility in water is highly dependent on the acidity of the carboxylic linker, which is in turn related to the presence of electron-withdrawing substituents on the aromatic ring, we speculate that less acidic linkers, such as BDC and NH<sub>2</sub>-BDC, fail to dissolve in the small amount of water contained in the Zr precursor, thus preventing crystallisation of the MOF from occurring. On the other hand, the higher water solubility of F<sub>4</sub>-BDC, NO<sub>2</sub>-BDC, Br-BDC allows the rapid reaction with hydrated Zr salts upon grinding and successive incubation at RT or 120 °C.

A different situation was encountered when the synthesis of Py-UiO-66 was attempted, which afforded nearly amorphous products using AcOH at both RT and 120 °C. We note that this linker features a highly acidic carboxylate (pK<sub>a1</sub> = 0.80) and a pyridinic N atom. As a consequence, PyDC is the only linker, among those tested here, able to form a zwitterion through proton transfer from the carboxylate to the pyridinic N atom. Thus, the presence of a deprotonated carboxylate makes it very prone to coordinate to the metal, with very fast crystallisation kinetics that lead to a poorly crystalline product. Therefore, according to a previous study where a large excess of concentrated HCl was employed to induce crystallisation of Py-UiO-66,<sup>45</sup> we decided to use concentrated HNO<sub>3</sub> (65 wt%) in place of AcOH. We chose to use HNO<sub>3</sub> in order to avoid the introduction of an additional species, i.e. chloride, in the reaction mixture. This strategy afforded a product with improved quality, but still not completely satisfactory (Figure 12S). Given the harsh conditions in which this

synthesis is performed, we speculated that prolonged heating could harm the product, therefore we attempted to reduce the reaction time down to 1 or 2 h. In both cases, highly crystalline products were recovered (Figure 12S). The  $^1\text{H}$  NMR spectra of the digested sample confirmed the purity of the compound and the eventual presence of nitrates into the structure (Figure 13S). Since the  $\text{HNO}_3$  solution already contains a high amount of water, the water screening was not carried out in this case.

The positive results obtained upon reduction of the reaction time with Py-UiO-66 prompted us to investigate if also other compounds could be obtained in a shorter time than the initial 24 h. We chose the most crystalline sample of every set of compounds ( $\text{F}_4$ -UiO-66 0  $\mu\text{L}$ ,  $\text{NO}_2$ -UiO-66 25  $\mu\text{L}$ , Br-UiO-66 100  $\mu\text{L}$ ) and reduced the reaction time down to 1 h and 2 h. The PXRD patterns of figure 14S demonstrate the formation of highly crystalline Br-UiO-66 also after 1 h or 2 h, while  $\text{F}_4$ -UiO-66 and  $\text{NO}_2$ -UiO-66 can be achieved but display low crystallinity. This is likely due to the slower crystallisation kinetics for the syntheses carried out at RT, which require a longer time to reach completion.

To check the possibility of getting good quality compounds on a larger scale, the synthesis of  $\text{F}_4$ -UiO-66 was scaled-up in two steps. The synthesis was initially attempted using 4 mmol each of  $\text{F}_4$ -BDC and  $\text{Zr}(\text{NO}_3)_4 \cdot 5\text{H}_2\text{O}$  and 4 mL of AcOH by milling for 1 h at 30 Hz, observing formation of a UiO-66 phase with low crystallinity and porosity (Figures 15Sa-16Sa). In a successive attempt, where the vessel was kept sealed for 24 h after initial milling, 1.5 g of a well crystallized compound was obtained, whose crystallinity is comparable to that obtained using 1 mmol of reagents (Figure 15Sb). This product displays BET s.a. of 888  $\text{m}^2\text{g}^{-1}$  and micropore volume of 0.33  $\text{cm}^3\text{g}^{-1}$ , about the same of that measured for the MOF obtained with the small scale synthesis (Figure 16Sb). Finally, a last synthesis employing 10 mmol of reagents ( $\text{F}_4$ -BDC and  $\text{Zr}(\text{NO}_3)_4 \cdot 5\text{H}_2\text{O}$ ) was carried out by just mixing them in a mortar and bypassing the milling step (see experimental section). Almost 4 g of good quality MOF (Figure 17S) was obtained, demonstrating the easy scalability of the procedure up to a 10-fold scale.

## Conclusions

We have reported a simple “shake ‘n bake” procedure for the synthesis of a range of functionalised Zr-based UiO-66 MOFs starting from commercial  $\text{Zr}^{\text{IV}}$  precursors. The method involves mixing of metal salt, linker, and a liquid reagent in a ball mill, followed by incubation of the mixture at either RT or 120  $^\circ\text{C}$ . We demonstrated the efficacy of the procedure for the synthesis when using functionalized carboxylic ligands with higher acidity and water solubility than simple terephthalic acid. The syntheses are quick and afford pure compounds with comparable crystallinity and porosity as those obtained by conventional solvothermal synthesis. Scalability was also proven to be effective up to 10-fold. This method allows to avoid toxic solvents and adds up to the range of existing approaches for the sustainable synthesis of MOFs for industrial applications.

## ASSOCIATED CONTENT

**Supporting Information.** XRPD patterns of MOFs and linkers, TGA curves, SEM images,  $\text{N}_2$  adsorption and desorption isotherms,  $^1\text{H}$ -NMR spectra, XRPD and BET curves for scale up syntheses “This material is available free of charge via the Internet at <http://pubs.acs.org>.”

## AUTHOR INFORMATION

### Corresponding Author

\* Ferdinando Costantino, [ferdinando.costantino@unipg.it](mailto:ferdinando.costantino@unipg.it)

\* Marco Taddei, [marco.taddei@unipi.it](mailto:marco.taddei@unipi.it)

### Present Addresses

†International Iberian Nanotechnology Laboratory, Avenida Mestre José Veiga s/n, 4715-330 Braga, Portugal.

### Author Contributions

The manuscript was written through contributions of all authors. / All authors have given approval to the final version of the manuscript. /

### Funding Sources

Any funds used to support the research of the manuscript should be placed here (per journal style).

## Acknowledgement

The authors acknowledge the European Union’s Horizon 2020 research and innovation programme under the Marie Skłodowska-Curie grant agreement No 663830 (M.T.), and the Engineering and Physical Sciences Research Council (EPSRC) for funding through the First Grant scheme EP/R01910X/1 (M.T. and M.J.M.). F.C, R.D. and F.M. thank Fondo Ricerca di Base (FRB2017) and the Project AMIS, University of Perugia for financial support.

## REFERENCES

- (1) Reinsch, H. “Green” Synthesis of Metal-Organic Frameworks. *Eur. J. Inorg. Chem.* **2016**, *2016* (27), 4290–4299. <https://doi.org/10.1002/ejic.201600286>.
- (2) Wang, S.; Serre, C. Toward Green Production of Water-Stable Metal-Organic Frameworks Based on High-Valence Metals with Low Toxicities. *ACS Sustain. Chem. Eng.* **2019**, *7* (14), 11911–11927. <https://doi.org/10.1021/acssuschemeng.9b01022>.
- (3) Julien, P. A.; Mottillo, C.; Friščić, T. Metal-Organic Frameworks Meet Scalable and Sustainable Synthesis. *Green Chem.* **2017**, *19* (12), 2729–2747. <https://doi.org/10.1039/c7gc01078h>.

- (4) Bennett, T. D.; Horike, S. Liquid, Glass and Amorphous Solid States of Coordination Polymers and Metal–Organic Frameworks. *Nat. Rev. Mater.* **2018**, *3* (11), 431–440. <https://doi.org/10.1038/s41578-018-0054-3>.
- (5) Adil, K.; Belmabkhout, Y.; Pillai, R. S.; Cadiou, A.; Bhatt, P. M.; Assen, A. H.; Maurin, G.; Eddaoudi, M. Gas/Vapour Separation Using Ultra-Microporous Metal-Organic Frameworks: Insights into the Structure/Separation Relationship. *Chem. Soc. Rev.* **2017**, *46* (11), 3402–3430. <https://doi.org/10.1039/c7cs00153c>.
- (6) Mason, J. A.; Veenstra, M.; Long, J. R. Evaluating Metal-Organic Frameworks for Natural Gas Storage. *Chem. Sci.* **2014**, *5* (1), 32–51. <https://doi.org/10.1039/c3sc52633j>.
- (7) Chen, Z.; Adil, K.; Weseliński, Ł. J.; Belmabkhout, Y.; Eddaoudi, M. A Supermolecular Building Layer Approach for Gas Separation and Storage Applications: The Eea and Rtl MOF Platforms for CO<sub>2</sub> Capture and Hydrocarbon Separation. *J. Mater. Chem. A* **2015**, *3* (12), 6276–6281. <https://doi.org/10.1039/c4ta07115h>.
- (8) Mondloch, J. E.; Katz, M. J.; Isley, W. C.; Ghosh, P.; Liao, P.; Bury, W.; Wagner, G. W.; Hall, M. G.; Decoste, J. B.; Peterson, G. W.; et al. Destruction of Chemical Warfare Agents Using Metal-Organic Frameworks. *Nat. Mater.* **2015**, *14* (5), 512–516. <https://doi.org/10.1038/nmat4238>.
- (9) Yang, D.; Gates, B. C. Catalysis by Metal Organic Frameworks: Perspective and Suggestions for Future Research. *ACS Catal.* **2019**, *9* (3), 1779–1798. <https://doi.org/10.1021/acscatal.8b04515>.
- (10) Cadiou, A.; Belmabkhout, Y.; Adil, K.; Bhatt, P. M.; Pillai, R. S.; Shkurenko, A.; Martineau-Corcoss, C.; Maurin, G.; Eddaoudi, M. Molecular Sorption: Hydrolytically Stable Fluorinated Metal-Organic Frameworks for Energy-Efficient Dehydration. *Science (80-. )*. **2017**, *356* (6339), 731–735. <https://doi.org/10.1126/science.aam8310>.
- (11) Chen, Z.; Li, P.; Zhang, X.; Li, P.; Wasson, M. C.; Islamoglu, T.; Stoddart, J. F.; Farha, O. K. Reticular Access to Highly Porous Acs-MOFs with Rigid Trigonal Prismatic Linkers for Water Sorption. *J. Am. Chem. Soc.* **2019**, *141* (7), 2900–2905. <https://doi.org/10.1021/jacs.8b13710>.
- (12) Escorihuela, J.; Narducci, R.; Compañ, V.; Costantino, F. Proton Conductivity of Composite Polyelectrolyte Membranes with Metal-Organic Frameworks for Fuel Cell Applications. *Adv. Mater. Interfaces* **2019**, *6* (2), 1–30. <https://doi.org/10.1002/admi.201801146>.
- (13) Wu, M. X.; Yang, Y. W. Metal–Organic Framework (MOF)-Based Drug/Cargo Delivery and Cancer Therapy. *Adv. Mater.* **2017**, *29* (23), 1–20. <https://doi.org/10.1002/adma.201606134>.
- (14) Cavka, J. H.; Jakobsen, S.; Olsbye, U.; Guillou, N.; Lamberti, C.; Bordiga, S.; Lillerud, K. P. A New Zirconium Inorganic Building Brick Forming Metal Organic Frameworks with Exceptional Stability. *J. Am. Chem. Soc.* **2008**, *130* (42), 13850–13851. <https://doi.org/10.1021/ja8057953>.
- (15) Farha, O. K.; Yazaydin, A. Ö.; Eryazici, I.; Malliakas, C. D.; Hauser, B. G.; Kanatzidis, M. G.; Nguyen, S. T.; Snurr, R. Q.; Hupp, J. T. De Novo Synthesis of a Metal-Organic Framework Material Featuring Ultrahigh Surface Area and Gas Storage Capacities. *Nat. Chem.* **2010**, *2* (11), 944–948. <https://doi.org/10.1038/nchem.834>.
- (16) Feng, D.; Gu, Z. Y.; Li, J. R.; Jiang, H. L.; Wei, Z.; Zhou, H. C. Zirconium-Metalloporphyrin PCN-222: Mesoporous Metal-Organic Frameworks with Ultrahigh Stability as Biomimetic Catalysts. *Angew. Chemie - Int. Ed.* **2012**, *51* (41), 10307–10310. <https://doi.org/10.1002/anie.201204475>.
- (17) Jiang, J.; Gándara, F.; Zhang, Y. B.; Na, K.; Yaghi, O. M.; Klemperer, W. G. Superacidity in Sulfated Metal-Organic Framework-808. *J. Am. Chem. Soc.* **2014**, *136* (37), 12844–12847. <https://doi.org/10.1021/ja507119n>.
- (18) Leubner, S.; Zhao, H.; Velthoven, N. Van; Henrion, M.; Reinsch, H.; Vos, D. E. De; Kolb, U.; Stock, N. Expanding the Variety of Zirconium-Based Inorganic Building Units for Metal – Organic Frameworks. **2019**, 11111–11116. <https://doi.org/10.1002/ange.201905456>.
- (19) Czaja, A. U.; Trukhan, N.; Müller, U. Industrial Applications of Metal–Organic Frameworks. *Chem. Soc. Rev.* **2009**, *38* (5), 1284–1293. <https://doi.org/10.1039/b804680h>.
- (20) Bai, Y.; Dou, Y.; Xie, L. H.; Rutledge, W.; Li, J. R.; Zhou, H. C. Zr-Based Metal-Organic Frameworks: Design, Synthesis, Structure, and Applications. *Chem. Soc. Rev.* **2016**, *45* (8), 2327–2367. <https://doi.org/10.1039/c5cs00837a>.
- (21) Venturi, D. M.; Campana, F.; Marmottini, F.; Costantino, F.; Vaccaro, L. Extensive Screening of Green Solvents for Safe and Sustainable UiO-66 Synthesis. *ACS Sustain. Chem. Eng.* **2020**, *8* (46), 17154–17164. <https://doi.org/10.1021/acssuschemeng.0c05587>.
- (22) Pakamore, I.; Rousseau, J.; Rousseau, C.; Monflier, E.; Szilágyi, P. Á. An Ambient-Temperature Aqueous



- Synthesis of Zirconium-Based Metal-Organic Frameworks. *Green Chem.* **2018**, *20* (23), 5292–5298. <https://doi.org/10.1039/c8gc02312c>.
- (23) Dai, S.; Nouar, F.; Zhang, S.; Tissot, A.; Serre, C. One-Step Room-Temperature Synthesis of Metal(IV) Carboxylate Metal–Organic Frameworks. *Angew. Chemie - Int. Ed.* **2021**, *60* (8), 4282–4288. <https://doi.org/10.1002/anie.202014184>.
- (24) Avci-Camur, C.; Perez-Carvajal, J.; Imaz, I.; Maspoch, D. Metal Acetylacetonates as a Source of Metals for Aqueous Synthesis of Metal-Organic Frameworks. *ACS Sustain. Chem. Eng.* **2018**, *6* (11), 14554–14560. <https://doi.org/10.1021/acssuschemeng.8b03180>.
- (25) Friščič, T.; Jones, W. Recent Advances in Understanding the Mechanism of Cocrystal Formation via Grinding. *Cryst. Growth Des.* **2009**, *9* (3), 1621–1637. <https://doi.org/10.1021/cg800764n>.
- (26) Beldon, P. J.; Fábíán, L.; Stein, R. S.; Thirumurugan, A.; Cheetham, A. K.; Friščič, T. Rapid Room-Temperature Synthesis of Zeolitic Imidazolate Frameworks by Using Mechanochemistry. *Angew. Chemie* **2010**, *122* (50), 9834–9837. <https://doi.org/10.1002/ange.201005547>.
- (27) James, S. L.; Adams, C. J.; Bolm, C.; Braga, D.; Collier, P.; Frišcic, T.; Grepioni, F.; Harris, K. D. M.; Hyett, G.; Jones, W.; et al. Playing with Organic Radicals as Building Blocks for Functional Molecular Materials. *Chem. Soc. Rev.* **2012**, *41* (1), 413–447. <https://doi.org/10.1039/c1cs15171a>.
- (28) Julien, P. A.; Užarević, K.; Katsenis, A. D.; Kimber, S. A. J.; Wang, T.; Farha, O. K.; Zhang, Y.; Casaban, J.; Germann, L. S.; Etter, M.; et al. In Situ Monitoring and Mechanism of the Mechanochemical Formation of a Microporous MOF-74 Framework. *J. Am. Chem. Soc.* **2016**, *138* (9), 2929 - 2932. <https://doi.org/10.1021/jacs.5b13038>.
- (29) Huang, Y. H.; Lo, W. S.; Kuo, Y. W.; Chen, W. J.; Lin, C. H.; Shieh, F. K. Green and Rapid Synthesis of Zirconium Metal-Organic Frameworks: Via Mechanochemistry: UiO-66 Analog Nanocrystals Obtained in One Hundred Seconds. *Chem. Commun.* **2017**, *53* (43), 5818 - 5821. <https://doi.org/10.1039/c7cc03105j>.
- (30) Karadeniz, B.; Howarth, A. J.; Stolar, T.; Islamoglu, T.; Dejanović, I.; Tireli, M.; Wasson, M. C.; Moon, S. Y.; Farha, O. K.; Friščič, T.; et al. Benign by Design: Green and Scalable Synthesis of Zirconium UiO-Metal-Organic Frameworks by Water-Assisted Mechanochemistry. *ACS Sustain. Chem. Eng.* **2018**, *6* (11), 15841 - 15849. <https://doi.org/10.1021/acssuschemeng.8b04458>.
- (31) Užarević, K.; Wang, T. C.; Moon, S. Y.; Fidelli, A. M.; Hupp, J. T.; Farha, O. K.; Friščič, T. Mechanochemical and Solvent-Free Assembly of Zirconium-Based Metal-Organic Frameworks. *Chem. Commun.* **2016**, *52* (10), 2133 - 2136. <https://doi.org/10.1039/c5cc08972g>.
- (32) Fidelli, A. M.; Karadeniz, B.; Howarth, A. J.; Huskić, I.; Germann, L. S.; Halasz, I.; Etter, M.; Moon, S. Y.; Dinnebier, R. E.; Stilinović, V.; et al. Green and Rapid Mechanochemical Synthesis of High-Porosity NU- and UiO-Type Metal-Organic Frameworks. *Chem. Commun.* **2018**, *54* (51), 6999 - 7002. <https://doi.org/10.1039/c8cc03189d>.
- (33) Reinsch, H.; Bueken, B.; Vermoortele, F.; Stassen, I.; Lieb, A.; Lillerud, K. P.; De Vos, D. Green Synthesis of Zirconium-MOFs. *CrystEngComm* **2015**, *17* (22), 4070-4074. <https://doi.org/10.1039/c5ce00618j>.
- (34) Chen, Z.; Wang, X.; Noh, H.; Ayoub, G.; Peterson, G. W.; Buru, C. T.; Islamoglu, T.; Farha, O. K. Scalable, Room Temperature, and Water-Based Synthesis of Functionalized Zirconium-Based Metal-Organic Frameworks for Toxic Chemical Removal. *CrystEngComm* **2019**, *21* (14), 2409 - 2415. <https://doi.org/10.1039/C9CE00213H>.
- (35) Hu, Z.; Gami, A.; Wang, Y.; Zhao, D. A Triphasic Modulated Hydrothermal Approach for the Synthesis of Multivariate Metal - Organic Frameworks with Hydrophobic Moieties for Highly Efficient Moisture-Resistant CO<sub>2</sub> Capture. *Adv. Sustain. Syst.* **2017**, *1* (11), 1-12. <https://doi.org/10.1002/adsu.201700092>.
- (36) D' Amato, R.; Donnadio, A.; Carta, M.; Sangregorio, C.; Tiana, D.; Vivani, R.; Taddei, M.; Costantino, F. Water-Based Synthesis and Enhanced CO<sub>2</sub> Capture Performance of Perfluorinated Cerium-Based Metal-Organic Frameworks with UiO-66 and MIL-140 Topology. *ACS Sustain. Chem. Eng.* **2019**, *7* (1), 394 - 402. <https://doi.org/10.1021/acssuschemeng.8b03765>.
- (37) Ye, G.; Zhang, D.; Li, X.; Leng, K.; Zhang, W.; Ma, J.; Sun, Y.; Xu, W.; Ma, S. Boosting Catalytic Performance of Metal-Organic Framework by Increasing the Defects via a Facile and Green Approach. *ACS Appl. Mater. Interfaces* **2017**, *9* (40), 34937-34943. <https://doi.org/10.1021/acsami.7b10337>.
- (38) Taddei, M.; Tiana, D.; Casati, N.; Van Bokhoven, J. A.; Smit, B.; Ranocchiari, M. Mixed-Linker UiO-66: Structure-Property Relationships Revealed by a Combination of High-Resolution Powder X-Ray Diffraction and Density Functional Theory Calculations. *Phys. Chem. Chem. Phys.* **2017**, *19* (2), 1551-1559. <https://doi.org/10.1039/c6cp07801j>.

- (39) Taddei, M.; Wakeham, R. J.; Koutsianos, A.; Andreoli, E.; Barron, A. R. Post-Synthetic Ligand Exchange in Zirconium-Based Metal - Organic Frameworks: Beware of The Defects! *Angew. Chemie - Int. Ed.* **2018**, *57* (36), 11706 - 11710. <https://doi.org/10.1002/anie.201806910>.
- (40) Katz, M. J.; Brown, Z. J.; Colón, Y. J.; Siu, P. W.; Scheidt, K. A.; Snurr, R. Q.; Hupp, J. T.; Farha, O. K. A Facile Synthesis of UiO-66, UiO-67 and Their Derivatives. *Chem. Commun.* **2013**, *49* (82), 9449 - 9451. <https://doi.org/10.1039/c3cc46105j>.
- (41) Cliffe, M. J.; Wan, W.; Zou, X.; Chater, P. A.; Kleppe, A. K.; Tucker, M. G.; Wilhelm, H.; Funnell, N. P.; Coudert, F. X.; Goodwin, A. L. Correlated Defect Nanoregions in a Metal-Organic Framework. *Nat. Commun.* **2014**, *5* (May), 1 - 8. <https://doi.org/10.1038/ncomms5176>.
- (42) Taddei, M. When Defects Turn into Virtues: The Curious Case of Zirconium-Based Metal-Organic Frameworks. *Coord. Chem. Rev.* **2017**, *343*, 1 - 24. <https://doi.org/10.1016/j.ccr.2017.04.010>.
- (43) Kandiah, M.; Nilsen, M. H.; Usseglio, S.; Jakobsen, S.; Olsbye, U.; Tilset, M.; Larabi, C.; Quadrelli, E. A.; Bonino, F.; Lillerud, K. P. Synthesis and Stability of Tagged UiO-66 Zr-MOFs. *Chem. Mater.* **2010**, *22* (24), 6632-6640. <https://doi.org/10.1021/cm102601v>.
- (44) Garibay, S. J.; Cohen, S. M. Isoreticular Synthesis and Modification of Frameworks with the UiO-66 Topology. *Chem. Commun.* **2010**, *46* (41), 7700 - 7702. <https://doi.org/10.1039/c0cc02990d>.
- (45) Barkhordarian, A. A.; Kepert, C. J. Two New Porous UiO-66-Type Zirconium Frameworks; Open Aromatic N-Donor Sites and Their Post-Synthetic Methylation and Metallation. *J. Mater. Chem. A* **2017**, *5* (11), 5612-5618. <https://doi.org/10.1039/C6TA11005C>.

---

SYNOPSIS TOC Functionalized Zr-UiO-66 MOFs can be obtained with a new easy and quick procedure starting from physical mixture of reagents and a few amount of liquid modulators

